Spectroscopic Investigations of High-Power Laser-Induced Dielectric Breakdown in Gas Mixtures Containing Carbon Monoxide

Svatopluk Civiš,[†] Dagmar Babánková,[†,‡] Jaroslav Cihelka,[†,‡] Petr Sazama,[†] and Libor Juha*[,‡]

J. Heyrovsky Institute of Physical Chemistry, Academy of Sciences of the Czech Republic, Dolejskova 3, 182 23 Prague 8, Czech Republic, and Institute of Physics, Academy of Sciences of the Czech Republic, Na Slovance 2, 182 21 Prague 8, Czech Republic

Received: December 21, 2007; Revised Manuscript Received: May 11, 2008

Large-scale plasma was created in gas mixtures containing carbon monoxide by high-power laser-induced dielectric breakdown (LIDB). The composition of the mixtures used corresponded to a cometary and/or meteoritic impact into the Earth's early atmosphere. A multiple-centimeter-sized fireball was created by focusing a single 85 J, 450 ps near-infrared laser pulse into the center of a 15 L gas cell. The excited reaction intermediates that formed in various stages of the LIDB plasma chemical evolution were investigated by optical emission spectroscopy (OES) with temporal resolution. Special attention was paid to any OES signs of molecular ions. However, carbon monoxide cations were registered only if their production was enhanced by Penning ionization, i.e., excess He was added to the CO. The chemical consequences of laser-produced plasma generation in a $CO-N_2-H_2O$ mixture were investigated using high resolution Fourier-transform infrared absorption spectroscopy (FTIR) and gas chromatography (GC). Several simple inorganic and organic compounds were identified in the reaction mixture exposed to ten laser sparks. $H_2{}^{18}O$ was used to avoid possible contamination. The large laser spark triggered more complex reactivity originating in carbon monoxide than expected, when taking into account the strong triple bond of carbon monoxide causing typically inefficient dissociation of this molecule in electrical discharges.

I. Introduction

The standard theories of chemical evolution in the Earth's early atmosphere presume that the organic molecules necessary for life formation on Earth (like amino acids, nitrogen bases, sugars, lipids, etc.) were formed by the action of, for example, lightning discharge plasma or an extraterrestrial body impact. The laboratory simulations of the high-energy-density processes have been carried out in various models of the Earth's early atmosphere, from highly reducing[1–3] to the slightly reducing and neutral.[4–6] The simulations used both laser plasma and electric discharges; their comparison can be found in ref 7.

Chemical physics investigates primarily the relations between the parameters of such laboratory plasma and its chemical actions in mixtures simulating the chemistry of the Earth's early atmosphere. The identification of the reaction products and intermediates, together with the measuring of their concentrations in a time scale, gives us an idea of the mechanisms and yields of these reactions in different gaseous mixtures. Geochemists are provided in this way with information on the probability of the formation of organic molecules via the high-energy-content phenomena, within their considered models of the Earth's early atmosphere. These models can be assessed from the point of view of life formation probability. In addition to this, the purpose of the chemical-physics research into the described phenomenon is also to find the conditions under which the laboratory plasma is at its closest to the natural conditions.

In this article, we focus on the chemical manifestations of the laser plasma in a model mixture of molecular gases with a high content of carbon monoxide. A CO-dominant atmosphere may not have existed on the early Earth for a long period of time, due to the relatively high reactivity of CO with numerous other components of the system, e.g., H_2 and OH in the primitive atmosphere and OH^- in the early ocean.[8] However, several processes have been suggested and recognized,[5] which could lead to its temporary establishment at exactly the time when the organic compounds necessary for later life should have been formed. The lunar impact record shows a high flux of various bodies on the Earth−Moon system until 3.8 billion years ago. Thus the formation of the large amount of CO on Earth could have been connected with frequent high-velocity impacts of extraterrestrial bodies at that time. The CO production may have occurred in the three following ways:[5]

(1) Comets could have supplied CO directly.[9]

(2) All the carbonaceous material contained in the extraterrestrial body may have been oxidized by oxygen derived from silicates, to produce CO in the impact plume.

(3) Meteoritic iron evaporated in the atmosphere could have reduced atmospheric CO_2 to CO.

Miyakawa et al.[5] suggest that a CO-dominant atmosphere could have been built up by impacts of extraterrestrial bodies into the early Earth's atmosphere. The CO-rich atmosphere should have exhibited a transient character because of at least three sinks for CO molecules:

(a) a variety of atmospheric reactions leading to organic molecules.

(b) oxidation to CO_2 by hydroxyl radicals produced by water vapor photolysis[10,11]

(c) the reaction in alkaline aqueous solutions producing formic acid[8]

We have focused on the reaction described in (a). The dissociation energy of carbon monoxide is largely due to the

* Author to whom correspondence should be addressed. Phone: +420-266052741. Fax: +420-286890265. E-mail:juha@fzu.cz.
† J. Heyrovsky Institute of Physical Chemistry.
‡ Institute of Physics.

10.1021/jp712011t CCC: $40.75
Published on Web 07/17/2008

triple bond between the carbon and oxygen atoms. The results of experiments carried out so far show that the plasma initiation of atmospheric reactions involving CO and producing organic compounds (e.g., ref 12) seems to be less effective in comparison to the effect of the ionizing radiation (e.g., refs 5 and 13). Our main aim has been to find out whether this holds also for our method of initiation.[6,14,15]

In this work, we study the chemical effects of large laser sparks created by the focused beam of a high-power laser in carbon monoxide and its mixtures with other molecular gases which represent a model of Earth's transient early atmosphere rich in CO. Optical emission spectroscopy with temporal resolution (tr-OES) was used for the observation of the early phases of laser plasma evolution (the formation of transient species such as atoms, radicals and molecular ions). In addition to this, high-resolution FTIR spectrometry and gas chromatography (GC-FID/TCD) were used for the identification of stable products.

II. Experimental Section

Laser-induced dielectric breakdown was achieved in the molecular gaseous mixture using the high-power iodine photodissociation laser system PALS. A single pulse of radiation at a wavelength of 1.3152 μm (pulse duration of 400 ps and energy of several hundred Joules) was extracted behind the fourth amplifier of the system. The diameter of the laser beam behind the fourth amplifier was 15 cm. One pulse was delivered every 25 min. The fourth-amplifier beam was focused into a gas cell by a plano-convex lens with a diameter of 15 cm and a focal length of 25 cm. A pulse energy was typically of 100 J. Power losses due to NIR beam reflections at the focusing lens and the cell window did not exceed 15%.

For the static LIDB experiments, a 15 L glass cell was used. The shape of the cell body was that of a cross with length and width both of 40 cm, with four windows. The main-laser-beam entrance windows were made of 4 cm thick glass, with a diameter of 20 cm, and 1.5 cm thick inspection windows with a diameter of 10 cm served for the collecting of the OES signals. The windows were mounted onto the glass body with stainless-steel flanges and sealed with viton rings. The cell was mounted on a 1 cm thick dural platform for easier manipulation and positioning. The cell's body was equipped with two vacuum valves (ACE Glass, USA) for gas handling.

The clean glass cell (the main body of cell was oven-annealed at 450 °C) was evacuated to a pressure of 3×10^{-5} Torr and then filled with high-purity N_2 and CO gases up to the atmospheric pressure (1:1, CO, Linde 99.99%; N_2, Messer 99.996%). Twenty milliliters of deionized water (or 2 mL of ^{18}O labeled water (97%, Cambridge Isotope Laboratories) in the case of isotopic experiments) was poured into the cell during the gas filling procedure with help of a syringe. After filling, the cell was closed and transported to the laser facility.

The optical emission from LIDB plasmas entered directly into the entrance slit of the spectrometer; i.e., no focusing lens was used because of the high intensity of laser spark light emission. Two ruled gratings were switched in the spectrometer (MS257, Oriel), one for preview (150 lines/mm, width of measured spectra = 400 nm) and the second for high-resolution measurement (1200 lines/mm, width of measured spectra = 60 nm). The dispersed spectrum was detected by an intensified CCD camera (ICCD; iStar 720, Andor), with a resolution of 0.08 nm/pixel for the high-resolution grating. Spectral lines in a distance down to 0.2 nm have been distinguished if a very narrow entrance slit is used to prevent saturation of the camera.

The synchronization of the intensified CCD camera with the laser pulse was accomplished using a photodiode signal. The spectrum was integrated for a 1 s period after the trigger. Each spectrum presented in this article corresponds to a single laser shot gas exposure. Due to the risk of electrical interference on the ICCD head occurring in the high-power laser hall, the spectrometer was placed in a Faraday cage.

All above-mentioned apparatus and procedures are in more details described in our previous papers[6,14] and references cited therein.

The absorption spectra were measured with a Bruker IFS 120 Fourier-transform infrared spectrometer (Bruker, Germany), in the spectral interval of 1800−7000 cm^{-1} using an InSb semiconductor detector and 0.01 cm^{-1} spectral resolution. Detailed, high-resolution spectra were measured with a non-apodized resolution of 0.0035 cm^{-1} in a narrow spectral interval determined by interference filters. It was usually necessary to accumulate 100 scans to obtain a sufficient signal/noise ratio.

For measurement purposes, the gaseous mixture studied (before and after the laser spark generation) was transferred into a previously evacuated glass IR absorption spectrophotometry cell with a length of 30 cm, equipped with KBr windows. The optimal pressure for the high-resolution spectra measurement was chosen with regard to the minimal spectral broadening of individual rotation-vibration lines (usually 450 Pa).

Gas chromatography (GC Hewlett-Packard 6090) was used as a complementary technique for the analysis of the volatile products of reactions initiated in the mixture by a large laser spark. Two gaseous samples of the $CO-N_2-H_2O$ mixture were exposed to ten laser sparks and then trapped in liquid nitrogen. After that, they were simultaneously injected with 10-port valves. In the branch with a thermal conductivity detector (TCD), a Hysep column (packed column) was used for the retention and removal of organic compounds and water; columns of HP-Plot Q (30 m × 0.53 mm × 40 μm film thickness) and a Molecular sieve 5A (30 m × 0.53 mm × 25 μm film thickness) were used for the separation of CO, CO_2 and N_2O. HP-Plot Q separated CO_2 from CO and N_2O. The sixth port valve was used to bypass the column Molecular sieve 5A during the analysis of CO_2 on TCD. After the analysis of CO_2, the mixture containing CO and N_2O was separated with the column molecular sieve 5A and monitored on the TCD. Following conditions of the analysis were employed: Carrier gas He, pressure 20 psi, splitless mode, loop volume 1 mL, bypass of Molecular sieve 5A at 5.1−10.0 min, constant temperature 40 °C for 23 min, then temperature gradient 20 °C min^{-1} to 200 °C. In the second branch, a DG-200 column (packed column) was used for water removal. C_1-C_4 alkanes and alkenes were separated on an HP-Plot Al_2O_3 "M" column (50 m × 0.53 mm × 15 μm film thickness, carrier gas: He 7.9 mL.min^{-1}, constant flow mode, split ratio: 1:50, loop: 250 μL, constant temperature 40 °C for 23 min, then temperature gradient 20 °C min^{-1} to 200 °C) and monitored by a flame ionization detector (FID).

III. Results and Discussion

A. High-Resolution FTIR Absorption Spectroscopy. The 15 L cell was filled with a mixture of carbon monoxide and nitrogen up to atmospheric pressure and 20 mL of deionized water was poured into its bottom. The outer jacket of the cell was heated with a heating strip to 50 °C; therefore the partial pressure of water vapor inside the cell was 12.3 kPa. A small sample of the mixture (1 mL) was transferred into an IR absorption cell and the blank absorption spectra were measured using FTIR; see Figure 1a. The spectra showed rotation-vibration

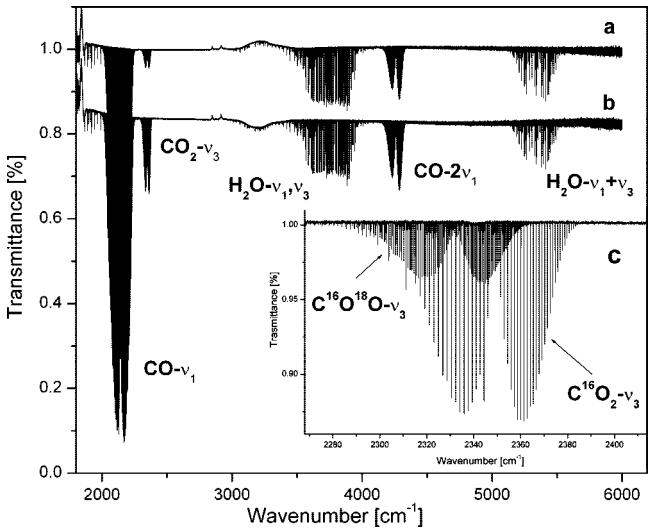

Figure 1. High-resolution FTIR absorption spectra of (a) an unirradiated CO−N_2−H_2O gaseous mixture, (b) the same mixture after ten laser sparks, and (c) the CO_2 band composed of spectral components belonging to the $C^{16}O^{18}O$ and $C^{16}O_2$ isotopomers.

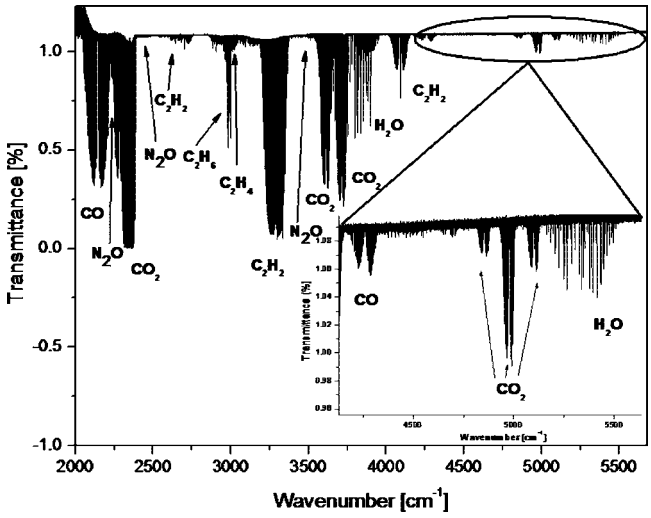

Figure 2. The FTIR absorption spectrum of the CO−N_2−H_2O mixture exposed to ten laser sparks and then trapped in liquid nitrogen.

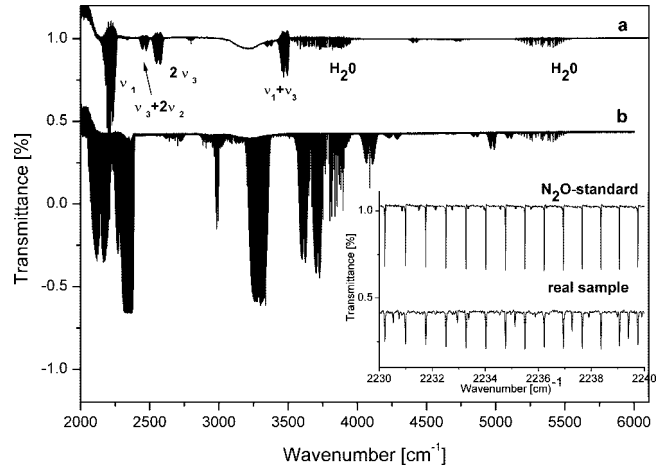

Figure 3. Comparison of the FTIR absorption spectra of (a) a N_2O standard and (b) the CO−N_2−H_2O mixture trapped in liquid nitrogen after its exposure to ten laser shots. The inset shows the comparison of the rotation structure of the ν_1 fundamental ro-vibration band in the real sample and in the N_2O standard.

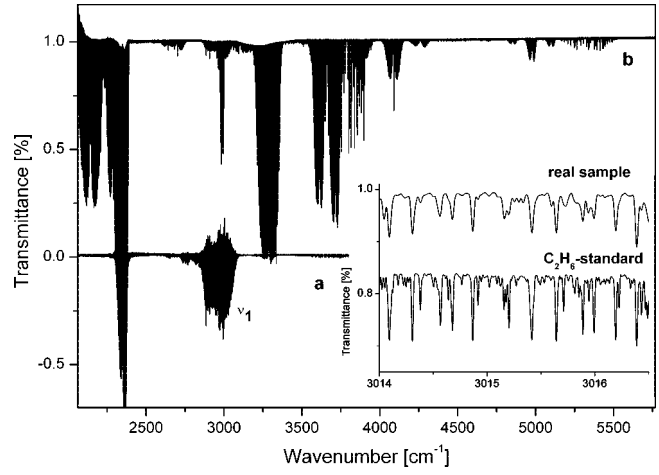

Figure 4. Comparison of the FTIR absorption spectra of (a) a C_2H_6 standard and (b) the CO−N_2−H_2O mixture trapped in liquid nitrogen after its exposure to ten laser shots. The inset shows the comparison of the rotation structure of the ν_1 fundamental ro-vibration band in the real sample and in the C_2H_6 standard.

(ro-vibration) bands of carbon monoxide, both fundamental and second harmonic frequencies, then two combination bands of water vapor, and also the third harmonic frequency of carbon dioxide.[16,17] The appearance of the carbon dioxide band was due to the presence of small carbon dioxide impurities (186.5 ppm) in the carbon monoxide gas.

The cell was then transported to the PALS facility and ten laser sparks were generated in the gaseous mixture. After the LIDB exposure, a sample of the gaseous mixture was again transferred from the irradiation cell into the IR cell. The IR absorption spectra (Figure 1b) of the exposed gas were measured using the FTIR spectrophotometer. The spectra showed a significant increase in intensity of the carbon dioxide rotation-vibration band caused by the action of laser sparks in the CO-N_2−H_2O gaseous mixture.

To remove the excess nitrogen and carbon monoxide from the gaseous mixture, the mixture was slowly pumped with a membrane pump through a nitrogen freezing trap. FTIR absorption spectra of the trapped and then evaporated gases were measured (Figure 2). Two rotation-vibration bands of nitrous oxide (N_2O) (Figure 3), and various bands of several simple hydrocarbons, apart from rotation-vibration bands of carbon monoxide (CO) and carbon dioxide (CO_2), were identified in the spectrum. From the hydrocarbons, there were namely ethane (Figure 4), ethylene (Figure 5), acetylene (Figure 6), and acetone (Figure 7). All compounds were identified on the basis of their comparison with the spectra of laboratory standards.

The four strongest bands seen in the spectrum belonged to acetylene. Two of these are assigned to the fundamental rotation-vibration frequencies, specifically ν_1 and ν_3, at 3374 and 3289 cm^{-1}, respectively. The remaining two bands at 4090 and 2642 cm^{-1} belong to higher harmonic or combination frequencies.[16,17] Only one rotation-vibration band of ethane at 2985 cm^{-1} was identified, belonging to its fundamental vibration frequency ν_{10}. For ethylene, four ro-vibration bands were identified, all belonging to the fundamental frequencies, ν_1, ν_5, ν_9 and ν_{11}, with centers at 3026, 3103, 3106 and 2989 cm^{-1} (refs 16 and 17).

Although the formation of small hydrocarbon molecules is in agreement with previous findings, N_2O has not yet been observed in nitrogen fixation experiments conducted with laser plasma (see, for example, ref 18 and, for a review, ref 15).

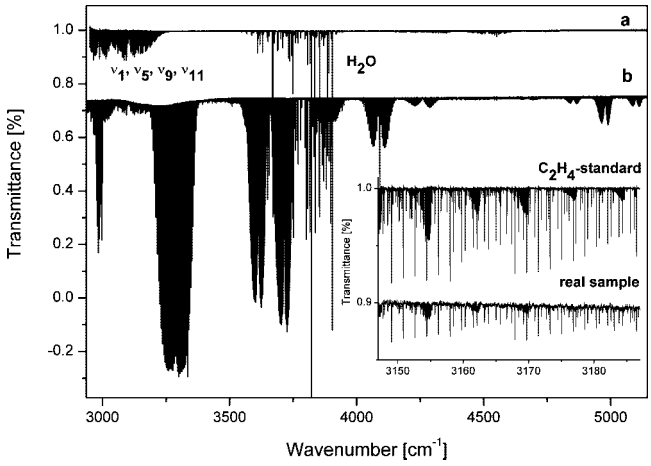

Figure 5. Comparison of the FTIR absorption spectra of (a) a C_2H_4 standard and (b) the $CO-N_2-H_2O$ mixture trapped in liquid nitrogen after its exposure to ten laser shots. The inset contains the comparison of the rotation structure in the real sample and in the C_2H_4 standard.

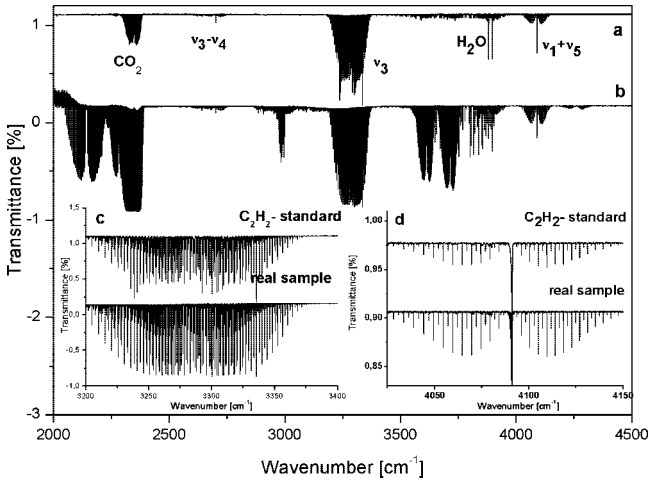

Figure 6. Comparison of the FTIR spectra of (a) a C_2H_2 standard and (b) the $CO-N_2-H_2O$ mixture trapped in liquid nitrogen after its exposure to ten laser shots. Insets show the comparison of the rotation structure of (c) the ν_3 fundamental and (d) $\nu_1 + \nu_5$ combination rovibration bands in the real sample and in the C_2H_2 standard.

Nevertheless, its formation was reported for example in a corona discharge in moist air.[19] This product was not expected to be found in the reaction mixture because of its low dissociation energy $D(N_2-O) = 1.7$ eV.[20,21] According to the intuitive stoichiometry argument, N_2O could be formed by the addition of an oxygen atom to a nitrogen molecule. However, the reaction (refs 18 and 20−22) occurs differently:

$$O + N_2 \rightarrow NO + N \quad (1)$$

Oxygen atoms are created in the mixture preferentially by the water dissociation because the triple bond in CO is much stronger than the single OH bond. Thus N_2O formed by the addition of an oxygen atom to a nitrogen molecule should be $N_2{}^{18}O$, if it is produced in the reaction mixture containing isotopically labeled water. However, only $N_2{}^{16}O$ was indicated in FTIR spectra measured in the present work.

The simple reaction paths leading to N_2O could be described by the following equations:

$$CO^* + N_2 \rightarrow N_2O + C(s) \quad (2)$$

$$NO^* + NO \rightarrow N_2O + O \quad (3)$$

Reaction 3 is well-known (see, for example, ref 20, p 175, and ref 23) whereas (2) has not yet been subjected to detailed

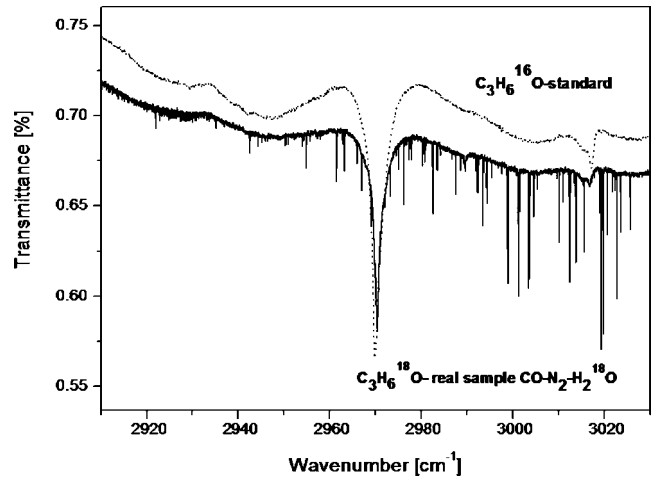

Figure 7. Comparison of the FTIR absorption spectra of (a) standard acetone,$(CH_3)_2C={}^{16}O$,and (b) the $CO-N_2-H_2{}^{18}O$ mixture trapped in liquid nitrogen after its exposure to ten laser shots.

investigation. In the Earth's contemporary atmosphere, nitrous oxide is considered[24–27] to be formed through the following reactions:

$$O(^1D) + N_2 + M \rightarrow N_2O + M \quad (4)$$

$$N + NO_2 \rightarrow N_2O + O \quad (5)$$

$$O_3^* + N_2 \rightarrow N_2O + O_2 \quad (6)$$

$$N_2(A^3\Sigma_\mu^+) + O_2 \rightarrow N_2O + O \quad (7)$$

However, reactions 6 and 7 could not take place in the $CO-N_2-H_2O$ mixture because of the negligible formation rate of O_2 and/or O_3 under our experimental conditions.

We may consider that N_2O is produced by some secondary processes, i.e., eqs 2–5, in the late stage of the chemical evolution of the LIDB plasma, because this molecule may be easily decomposed photochemically as well as thermally. NO and NO_2 are among the products of N_2O photolysis; they were not detected among the variety of products of LIDB exposure to the $CO-N_2-H_2O$ mixture. Therefore, N_2O is probably formed in the late phase of the laser spark expansion into the cold molecular gases when VUV emission of LIDB plasma becomes weak.

The formation of N_2O, which in conventional plasmachemistry is typical for glow and corona discharges in air[19] and CO_2-N_2,[28] could be explained in the present study by (a) a low oxygen content and strong oxygen bonding in the irradiated system and (b) by the expansion of the LIDB plasma into a large volume of cold molecular gas. The laser spark in our case is produced in the center of the 15 L gas cell so that the hot plasma is cooled down slowly, in a large volume. In smaller reactors, the plasma is quenched by collectors and/or walls located close to the plasma core; see for example ref 12. The much larger volumes of relatively cold plasma produced in the 15 L cell cause a product pattern more typical for a low temperature discharge plasma than for a high temperature one. Plasma quenching by a gas, not by a solid surface, is also closer to an evolution of a lightning channel and/or impact plasma occurring in a real planetary atmosphere.

High-resolution FTIR spectroscopy makes it possible to carry out a laser-plasma chemical experiment with stable isotope labeling. $H_2{}^{18}O$ ($[^{18}O] = 99.9\%$) was introduced into the mixture of CO and N_2 gases in the 15 L irradiation cell, instead of water with a natural isotope composition. The mixture was exposed

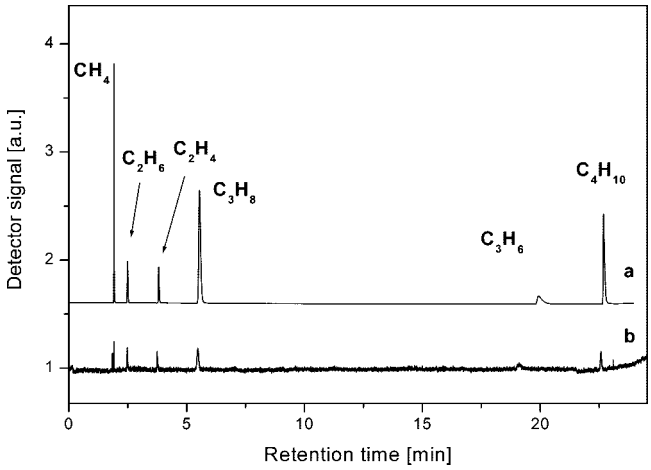

Figure 8. Comparison of gas chromatograms (FID signal) taken for (a) a mixture of standard hydrocarbons and (b) the $CO-N_2-H_2O$ mixture trapped in liquid nitrogen after its exposure to ten laser shots.

TABLE 1: Gaseous Products of LIDB-Initiated Reactions in $CO-N_2-H_2O$ Analyzed by Gas Chromatography

concentration	CO_2[a]	N_2O	CH_4	C_2H_6	C_2H_4	C_3H_8	C_3H_6	C_4H_{10}
ppm	559.5	0.81	0.24	0.1	0.1	0.16	0.09	0.08
10^{-6} g/L	1099	1.59	0.17	0.14	0.13	0.32	0.16	0.21

[a] 186.5 ppm (366.3×10^{-6} g/L) of CO_2 as an impurity from the pressure cylinder of CO.

to ten laser sparks and then investigated by the high-resolution FTIR absorption spectroscopy. A sample was frozen and after removing the excess nitrogen and carbon monoxide, it was quantitatively transferred into an IR absorption cell. The spectra of most of the organic compounds were identical to the previous spectra with unlabeled water, with the exception of the 2950−3020 cm^{-1} range, which is dominated by ν_1 and ν_{20} bands of acetone.[16,17] A reference spectrum of acetone with a natural isotopic composition was measured with a resolution of 0.0035 cm^{-1}. This spectrum was compared with the spectrum of acetone formed in a $CO-N_2-H_2{}^{18}O$ mixture exposed to ten laser sparks. The comparison of the two spectra in Figure 7 revealed the following band shifts in the sample obtained from the mixture with ^{18}O labeled water: ν_1 at 3018.5 cm^{-1} (CH_3 d-stretch a_1 symmetry[16]) exhibits a red shift of 0.5 cm^{-1}, ν_{20} at 2972 cm^{-1} (CH_3 d-stretch b_2 symmetry[16]) shows a blue shift of 0.5 cm^{-1}, which both belong to $(CH_3)_2C=^{18}O$, i.e., acetone labeled with the heaviest stable isotope of oxygen.[29] This could indicate that the acetone found in the irradiated mixture was synthesized from $H_2{}^{18}O$. The calculated shift of ν_{CO} (1732 cm^{-1}) frequency is about 29 cm^{-1} (ref 30) for the $(CH_3)_2C=^{18}O$ molecule and the calculations predict very small shifts (about 3 cm^{-1}) for the other carbonyl bands (carbonyl out-of-plane band). Therefore a weak influence of ^{18}O atom on the CH_3 symmetrical stretch vibration is expected. This is in good agreement with the shift of 0.5 cm^{-1} observed in our experiments.

However, there is also an unlikely possibility that the acetone was an impurity appearing in the sample during its preparation and handling and was labeled by an isotope exchange with $H_2{}^{18}O$. To test this hypothesis, we mixed 0.2 mL of acetone and 0.5 mL of $H_2{}^{18}O$ (99.9%) in a glass ampule. The ampule was sealed, heated, and kept at 80 °C for 180 h. After 180 h, the ampule was opened and the mixture was analyzed using high-resolution FTIR spectrophotometry in the same way as described above. No isotope exchange between the $(CH_3)_2C=^{16}O$ and $H_2{}^{18}O$ has been observed under these conditions. Thus conclusive evidence is given that the acetone found in the LIDB-exposed reaction mixture was formed due to the laser-plasmachemical reaction of water with other components of the mixture.

A detailed description of the individual spectral bands of isotopically labeled acetone in the range of ro-vibration bands ν_1 and ν_{20} requires detailed ab initio calculations and will be the subject of a following study. Within the framework of the experiments with ^{18}O-labeled water ($H_2{}^{18}O$), bands of $C^{16}O^{18}O$, $C^{18}O_2$, $C^{18}O$ and $H_2{}^{16}O$ molecules were observed next to the dominant basic rotation-vibration bands of $C^{16}O_2$, $C^{16}O$ and $H_2{}^{18}O$ in the spectra of the studied mixture after exposure. (Examples may be seen in Figure 1c; assignment and interpretation can be found in ref 29) Carbon dioxide formation is considered to be primarily governed by the reaction[11] between carbon monoxide molecules and hydroxyl radicals produced by dissociation of water vapor:

$$CO + OH \rightarrow CO_2 + H \quad (8)$$

However, the carbon monoxide disproportionation reaction[31] may also give carbon dioxide:

$$2CO \rightarrow CO_2 + C(s) \quad (9)$$

The study of the processes that can lead to the formation of all the above-described isotopomers will be the subject of our subsequent paper. Both the reactions of isotope exchange and of laser-plasma chemical type are observed. The latter are studied in relation to the delivered energy of the laser pulses.

B. Gas Chromatography. The gas chromatography analysis of LIDB-initiated mixture was used to confirm and quantify the above-mentioned FTIR findings. The results of GC analysis of products formed by ten laser sparks in the $CO-N_2-H_2O$ mixture, which were subsequently trapped in liquid nitrogen are shown in Figure 8 (FID signal) and summarized in Table 1. The high sensitivity of the method employed enables detection of ppm of CO, CO_2, and N_2O and tenths of ppm of C_1-C_4 hydrocarbons. In addition to CO, a high concentration of CO_2 and a medium concentration of N_2O were found in the LIDB-transformed mixture. Together with the FTIR spectrometry results, there is conclusive evidence of the efficient formation of these gases in $CO-N_2-H_2O$ mixture exposed to a large laser spark. Signal of the flame ionization detector at GC analysis of the transformed mixture and model mixture of C_1-C_4 alkanes and alkenes standards is shown in Figure 8. Peaks belonging to methane, ethane, ethylene, propane, propene, and butane were identified in the chromatogram of the mixture exposed to laser sparks. This indicates that a complex mixture of hydrocarbons was formed during LIDB of the $CO-N_2-H_2O$ gaseous mixture. In comparison with the FTIR absorption spectroscopy, the gas chromatography is the more sensitive method. Because of higher FTIR spectrophotometry detection limits, not all compounds detected by GC were identified by FTIR.

C. Time-Resolved Optical Emission Spectroscopy. Among the possible causes[15] of chemical changes in a laser-plasma-chemical system, (a) high energy photons (VUV, XUV, and X-ray radiation) and (b) highly charged ions and fast electrons, emitted from the hot core of a laser spark, may directly and efficiently induce the ionization of molecules in the gas surrounding the primary LIDB plasma. The surprising result of our previous spectroscopy investigations was that only the following transient species (namely those listed in Table 2) were detected:

TABLE 2: LIDB-Produced Chemical Species Detected in $CO/CO_2-N_2-H_2O$ with Different Diagnostic and Analytical Techniques

analytical/diagnostic technique (ref)	gas mixture	identified species
HPLC/MS (ref 6)	$CO_2-N_2-H_2O$	glycine, alanine, serine, asparagine
	$CO-N_2-H_2O$	alanine
otical ES (refs 6 and 14)	$CO_2-N_2-H_2O$	CN
	$CO-N_2-H_2O$	CN, C_2, C_3
X-ray ES (refs 14 and 32)	$CO-N_2$	N^{6+}, N^{5+}, O^{7+}, O^{6+}, C^{5+}, C^{4+}
FTIR (present work)	$CO-N_2-H_2O$	N_2O, C_2H_2, C_2H_4, C_2H_6, C_3H_6O
GC/FID (present work)	$CO-N_2-H_2O$	CH_4, C_2H_4, C_2H_6, C_3H_6, C_3H_8, C_4H_{10}
GC/TCD (present work)	$CO-N_2-H_2O$	CO_2, N_2O

(A) in the early stage of laser spark evolution ($t \sim \tau_{pulse}$), highly charged atomic ions in the hot, dense plasma of laser spark core[14,32]

(B) in the late stage of laser spark evolution ($t \gg \tau_{pulse}$), small radicals, single charged atomic ions, and neutral atoms.

We did not observe any signs of molecular ions, formed by the photoionization, charge-transfer and/or impact-ionization processes, in the optical-emission spectra of the laser spark in $CO/CO_2-N_2-H_2O$ gases. Therefore we conducted an experiment to test our experimental layout and OES diagnostics to detect molecular ions when their formation was enhanced by adding helium gas to satisfy the conditions of the Penning effect.[33]

Penning ionization experiments have already been carried out in our laboratory to increase the abundance of molecular ions in electrical discharges; e.g., see the earlier study focused on H_3^+ ions.[34] In the present study we are benefiting from the fact that He has significantly higher ionization potential (24.6 eV) than CO (13.99 eV, ref 35). Thus a collision of an electronically highly excited helium atom with a carbon monoxide molecule leads to the ionization of the molecule.

The studied CO gas was diluted with a high amount of helium (approximately 1:100) and irradiated by an 85 J laser pulse. The time-resolved UV−vis emission spectra were measured in a single-shot mode on the microsecond time scale with a spectral resolution of 0.08 nm/pixel using the high-resolution grating. The gas mixtures were investigated at atmospheric pressure and at a pressure of 33.3 kPa. During the exposure in the time interval of 1 μs to 1 s, an emission spectrum was measured in the 220−280 nm range (Figure 9). The spectrum revealed several bands, of which the band at 230 nm belonged to the $B^2\Sigma^+ \rightarrow X^2\Sigma^+$ (0,1) electron transition of the CO^+ ion (ref 36); two intensive lines at 248 and 251 nm belonged to the carbon and helium atoms, respectively. The latter coincided with the C^+ line, which also appeared at 275 nm.

The next step was to carry out detailed measurements in the 480−530 nm range, where the $A^2\Pi_{1/2}-X^2\Sigma^+$ (0,0) comet-tail emission subband of CO^+ should be located according to ref 37. This band is overlapped by the $1^3\Sigma^+-X^3\Pi$ (0,0) band of CO^{2+} around 492 nm. In addition, this spectral range also showed lines of neutral CO and atomic He at 504.8 nm, which coincides with the carbon atom line around 505.2 nm.

Time-resolved spectra in 10 μs steps were measured afterward in the 490−530 nm range; see Figure 10. The most distinctive lines in the first 10 μs are the triplet transition of CO (probably

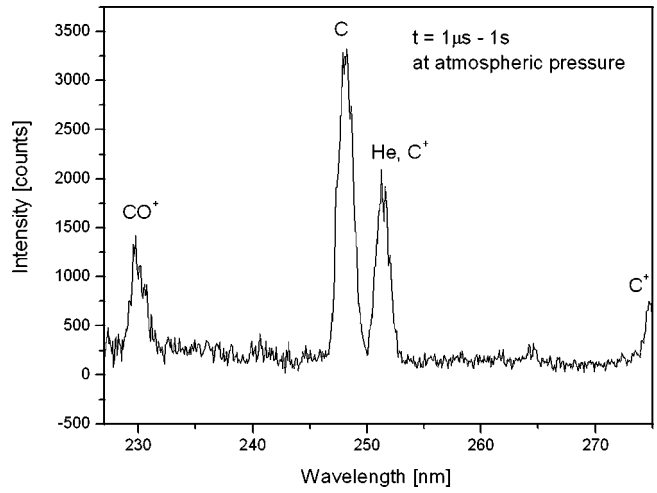

Figure 9. Ultraviolet emission spectrum of the late evolution ($t > 1$ μs) of a large laser spark in the CO−He (1:100) mixture at atmospheric pressure.

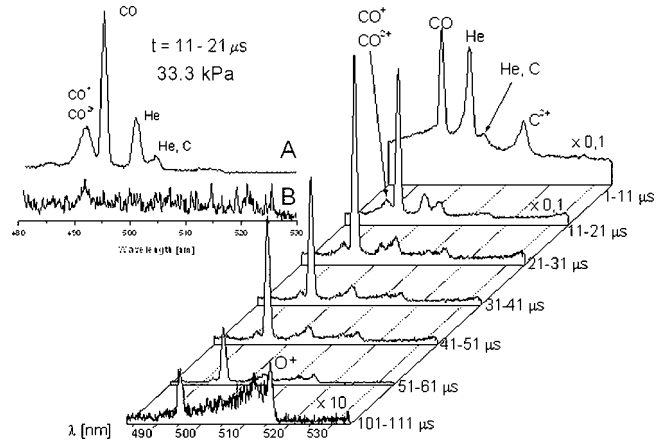

Figure 10. Time-resolved OES spectra of LIDB in the He−CO mixture (100:1) at a total pressure of 33.3 kPa.

its $d^3\Delta_2-a^3\Pi_1$ (11,2) band), the atomic line of He and probably the $1s^22s5p-1s^22s7s$ line of C^{2+} at 515 nm.

Figure 11 shows the temporal evolution of the He line at 501.6 nm and the CO^+ and CO^{2+} bands at 492.5 nm, recorded in 10 μs intervals. The 501.6 nm He line (1s2s−1s3p) shows very fast collision relaxation, as seen in Figure 10 and Figure 11. The corresponding lifetime of the line is 3.5 μs. In contrast to that, the lines corresponding to CO^+ a CO^{2+} appear in the spectrum after 10 μs.

The chemical processes in He/CO plasma that can lead to the formation and the decay of CO^+ can be described in the following way:

$$He + e_{fast} \rightarrow He^* + e_{slow} \quad (10)$$

$$He^* + CO \rightarrow CO^+ + e^- + He \quad (11)$$

Belic et al.[38] discussed one electron ejection from CO^+ ions via Franck−Condon transitions, which leads to purely dissociative states or to doubly charged CO^{2+} ions that are metastable against dissociation; a similar mechanism may be considered for double charge ion formation:

$$He^* + CO^+ \rightarrow CO^{2+} + e^- + He \quad (12)$$

The different additional dissociative channels to be considered are

$$e^- + CO^+ \rightarrow C^+ + O^+ + 2e^- \quad (13)$$

$$\rightarrow C^{2+} + O + 2e^- \quad (14)$$

$$\rightarrow O^{2+} + C + 2e^- \quad (15)$$

$$e^- + CO^{2+} \rightarrow C^+ + O^+ + e^- \quad (16)$$

The formation of a pair of singly charged ions - symmetrical dissociation (13), the formation of double charged atomic ions produced together with a neutral C or O atom by asymmetrical dissociation (14) and (15). Belic et al.[38] presented experimentally obtained absolute cross-reaction measurements for electron impact ionization reaction, asymmetrical dissociative ionization channels (14) and (15). Kim and Irikura[39] calculated total ionization cross-sections for several positive ions including CO^+. For many ions the theory was in good agreement with experimental data measured by Belic et al.[38] but in the case of the CO^+ ion, the experimentally obtained data were much lower than the theory. This large difference between the theory and experiment on CO^+ is in all probability a strong indication of the dominance of the dissociative ionization channel (13), which was not included in the interpretation of Belic's experiments.[38]

In our time-resolved spectra, we observed a composed band at 492.5 nm, which may be assigned to the $A^2\Pi-X^2\Sigma^+$ bands of CO^+ and the $1^3\Sigma^+-X^3\Pi$ bands of CO^{2+} ions. Cossart et al.[37] provided a hypothesis about the predissociation of upper $1^3\Sigma^+$ through the spin -orbit coupling with a repulsive $1^3\Sigma^-$ state. Larsson et al.[40] calculated that the predissociation lifetime of $1^3\Sigma^+$ is shorter than 1 μs. The Cossart hypothesis is based on the fact that the transition lifetimes for the $A^2\Pi-X^2\Sigma^+$ bands of CO^+ are about 3 μs (see ref 41), whereas the corresponding lifetimes for the $1^3\Sigma^+-X^3\Pi$ bands of the CO^{2+} band should be about twice as long. In the experiments of Belic et al.,[38] the products of CO^{2+} dications needed about 9 μs to reach the detector. Therefore, only the dications with a lifetime larger than this value were detected.

Based on the above-given facts, the processes of carbon monoxide molecular ion formation in the CO−He plasma are represented by eqs 11 and 12. The ion extinction mechanism is described by eqs 13–16. The intensity of He, CO^{2+}, O^+ and C^+ lines against time in the microsecond scale, as extracted from the optical emission spectra of LIDB plasma in the visible spectral range, is presented in Figure 11. The lifetime of the He I excited state [1s2s−1s3p], is estimated from the fit of the exponential decay which corresponds to 3.4 μs. During this time, helium exchanges the energy by collisions with molecules of CO. The single ionization threshold of the CO determined by Belic et al.[38] corresponds to 14 eV. In the experiment carried out by G. Dawber et al.,[42] the CO^{2+} appearance potential (in the $^3\Pi$, $v = 0$ state) relative to the $v = 0$ of the ground $X^1\Sigma$ state of neutral CO was determined to be 41.29 eV. The difference between this value and the CO single ionization threshold gives the value of 27.3 eV for the CO^+ ionization threshold.

In our spectra, after 10 μs, a band with an approximate lifetime of 12.9 (1.6) μs appears at 492.5 nm, which could belong to CO^+ or CO^{2+}. The theoretically obtained and theoretically predicted longer lifetimes support the hypothesis of $1^3\Sigma^+-X^3\Pi$ bands of CO^{2+}.

As has been mentioned above, Kim and Irikura[39] proved that the dissociative channel CO^+ (13), originally rejected by Belic et al.,[38] plays an important role. The atomic lines of O^+ and C^+ are created in this symmetrical dissociation process. In our case also, the band dissociation at 492.5 nm produces O^+ (515.9 nm) and C^+ (512.2 nm) with lifetimes of 18.9(2.2) and 27.1(5.4) μs, respectively (see Figure 11). The simultaneous detection of both lines halfway through the 492.5 nm line dissociation supports the symmetrical dissociation theory. Unfortunately, a similar dissociation process and the same fragments can be expected both with CO^+ and CO^{2+} (13) and (16). On the basis of the experimentally obtained lifetimes and their comparison with the calculations of transition moments for CO^+ and CO^{2+} (ref 37), the corresponding lifetimes for the $1^3\Sigma^+-X^3\Pi$ bands of CO^{2+} in the same spectral region should be about twice as long as the result of transition moment calculation for CO^+. We would therefore be inclined to conclude that the band at 492.5 nm belongs to the dication of CO^{2+}. However, it is necessary to take into account that the ionization energy of the helium atom is only 24.6 eV, i.e., slightly lower than the first ionization threshold of CO^+ (27.3 eV). The question remains whether the highly excited helium atoms have sufficient energy for the Penning ionization of CO^+ to CO^{2+} (12). However, the CO^+ ions in the considered system are also in a state of rather high electronic excitation (see Figure 9), thus from the energetic point of view, this type of ionization is possible.

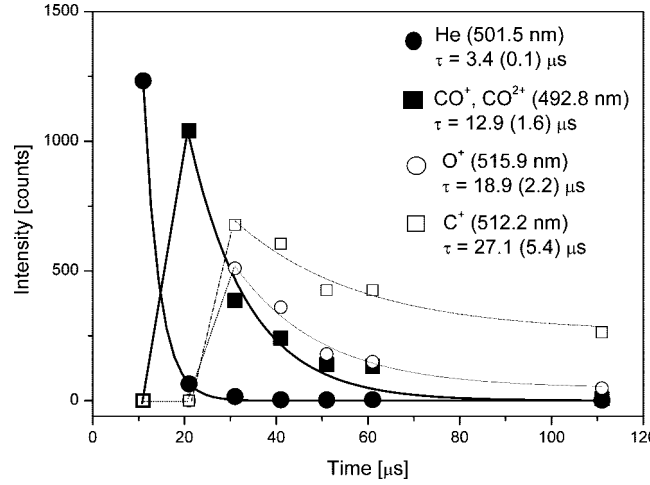

Figure 11. Temporal evolution of line intensities of He [1s2s−1s3p], CO^+, O^+ [$2s^22p^2(^3P)3p-2s^22p^2(^3P)3d$] and C^+ [$2s2p(^3P^\circ)-2s2p(^3P^\circ)3p$] electronic transition in an expanding laser spark produced by a high-power laser system in the He−CO mixture (100:1) at a total pressure of 33.3 kPa.

These results show that we are able to detect molecular ions if they are present in the laser spark system. The experiment raised the question of why we do not detect any molecular ions by means of their molecular emission spectra in the case of a helium-free mixture, i.e., when the Penning ionization is turned out. The explanation which assumes that the rates of photo-, impact-, and charge-transfer ionization are too low to exceed the OES detection limit of formed species seems unlikely. More likely is the explanation that the direct molecular ionization processes occur immediately after the optical breakdown of the gaseous mixture. In this case, a narrower temporal window for collecting OES records should be applied shortly after the laser pulse passes through the gas. However, strong atomic, ionic and blackbody emission from the core of LIDB plasma could, in some systems, make this measurement impossible.

IV. Concluding Remarks

The results of our earlier experiments with large laser sparks (ref 6 Table 2) indicated that carbon monoxide in model atmosphere produced a less complex product pattern for the amino-acid formation than the gas mixtures containing other possible constituents of our historical planetary atmospheres,

e.g., carbon dioxide. However, the results of our present work (Table 2), focused on the formation of small-molecule volatile products, are encouraging, in terms of both the quality and the quantity of such products formed in the mixtures containing CO, which are the laboratory simulations of the possible transient CO-rich types of the planetary atmosphere.

In such an atmosphere, not only the nitrogen fixation, following reaction paths that result in the formation of nitrous oxide, but also the synthesis of volatile organic compounds could have occurred. In addition, carbon dioxide production is efficiently initiated by high-energy density phenomena in an atmosphere composed of carbon monoxide, nitrogen and water vapor. Thus the transient atmosphere could have been quickly transformed by lightning and related phenomena into the standard oxidation composition.

Optical emission spectra do not indicate the formation of molecular ions connected with the formation and evolution of the large laser spark in the CO-rich mixture. Although it could testify to the key role of thermal and shock waves in the chemistry of the spark under the given experimental conditions, the secondary ionization processes cannot yet be rejected. In the present work, the generation of molecular ions (CO^+ and CO^{2+}) by Penning ionization satisfactorily proved that our experimental layout and diagnostics are able to investigate such phenomena. A systematic search for molecular ions, conducted closely to the LIDB core in time as well as in space, is required to give the final answer to this question.

Acknowledgment. This work was funded by the Grant Agency of the Czech Republic, grant No. 203/06/1278. During our experiments, the PALS facility was operated with the partial financial support of the Czech Ministry of Education, grant LC528.

References and Notes

(1) Miller, S. L. *Science* **1953**, *117*, 147.
(2) Miller, S. L. *J. Am. Chem. Soc.* **1955**, *77*, 2351.
(3) Urey, H. C. *Proc. Nat. Acad. Sci. U.S.A.* **1952**, *38*, 351.
(4) Schlesinger, G.; Miller, S. L. *J. Mol. Evol.* **1983**, *19*, 376.
(5) Miyakawa, S.; Yamanashi, H.; Kobayashi, K.; Cleaves, H. J.; Miller, S. L. *Proc. Natl. Acad. Sci. U.S.A.* **2002**, *99*, 14628.
(6) Civiš, S.; Juha, L.; Babánková, D.; Cvačka, J.; Frank, O.; Jehlička, J.; Králiková, B.; Krása, J.; Kubát, P.; Muck, A.; Pfeifer, M.; Skála, J.; Ullschmied, J. *Chem. Phys. Lett.* **2004**, *386*, 169.
(7) Scattergood, T. W.; McKay, C. P.; Borucki, W. L.; Giver, L. P.; Van Ghyseghem, H.; Parris, J. E.; Miller, S. L. *Icarus* **1989**, *81*, 413.
(8) Van Trump, J. E.; Miller, S. L. *Earth Planet. Sci. Lett.* **1973**, *20*, 145.
(9) Cottin, H.; Gazeau, M. C.; Raulin, F. *Planet. Space Sci.* **1999**, *47*, 1141, and references cited therein.
(10) Bar-Nun, A.; Hartman, H. *Orig. Life* **1978**, *9*, 93.
(11) Bar-Nun, A.; Chang, S. *J. Geophys. Res.* **1983**, *88*, 6662.
(12) Miyakawa, S.; Sawaoka, A. B.; Ushio, K.; Kobayashi, K. *J. Appl. Phys.* **1999**, *85*, 6853.
(13) Kobayashi, K.; Kaneko, T.; Saito, T. *Adv. Space Res.* **1999**, *24*, 461.
(14) Babánková, D.; Civiš, S.; Juha, L.; Bittner, M.; Cihelka, J.; Pfeifer, M.; Skála, J.; Bartnik, A.; Fiedorowicz, H.; Mikolajczyk, J.; Ryć, L.; Šedivcová, T. *J. Phys. Chem. A* **2006**, *110*, 12113.
(15) Babánková, D.; Civiš, S.; Juha, L. *Prog. Quantum Electron.* **2006**, *30*, 75.
(16) http://cfa-www.harvard.edu/hitran/.
(17) Guelachvili, G.; Rao, K. N. *Handbook of Infrared Standards*; Academic Press; New York, 1986.
(18) Navarro-González, R.; McKay, C. P.; Mvondo, D. N. *Nature* **2001**, *412*, 61.
(19) Bhetanabhotla, M. N.; Crowell, B. A.; Coucouvinos, A.; Hill, R. D.; Rinken, R. G. *Atmos. Environ.* **1985**, *19*, 1391, and references cited therein.
(20) Okabe, H. *Photochemistry of Small Molecules*; Wiley; New York, Chichester, Brisbane, Toronto, 1978 (see also references cited therein).
(21) Yung, Y. L.; DeMore, W. B. *Photochemistry of Planetary Atmospheres*; Oxford University Press; New York, Oxford, 1999. (see also references cited therein).
(22) Yung, Y. L.; McElroy, M. B. *Science* **1979**, *203*, 1002.
(23) Borucki, W. J.; Chameides, W. L. *Rev. Geophys. Space Phys.* **1984**, *22*, 363.
(24) Malcolme-Lawes, D. J. *Nature* **1974**, *247*, 540.
(25) Zipf, E. C. *Nature* **1980**, *287*, 523.
(26) Prasad, S. S. *Nature* **1981**, *289*, 386.
(27) Iannuzzi, M. P.; Jeffries, J. B.; Kaufman, F. *Chem. Phys. Lett.* **1982**, *87*, 570.
(28) Nna-Mvondo, D.; Navarro-González, R.; Raulin, F.; Coll, P. *Orig. Life Evol. Biosph.* **2005**, *35*, 401, and references cited therein.
(29) Pinchas, S.; Laulicht, J. *Infrared Spectra of Labeled Compounds*; Academic Press; London, 1972; chapter 7 and references cited therein.
(30) Davis, R. E.; Grosse, D. J. *Tetrahedron* **1970**, *26*, 1171.
(31) Essenhigh, K. A.; Utkin, Y. G.; Bernard, C.; Adamovich, I. V.; Rich, J. W. *Chem. Phys.* **2006**, *330*, 506, and references cited therein.
(32) Davídková, M.; Juha, L.; Bittner, M.; Koptyaev, S.; Hájková, V.; Krása, J.; Pfeifer, M.; Štísová, V.; Bartnik, A.; Fiedorowicz, H.; Mikolajczyk, J.; Ryc, L.; Pína, L.; Horváth, M.; Babánková, D.; Cihelka, J.; Civiš, S. *Radiat. Res.* **2007**, *168*, 382.
(33) Penning, F. M. *Naturwiss.* **1927**, *15*, 818.
(34) Civis, S.; Kubat, P.; Nishida, S.; Kawaguchi, K. *Chem. Phys. Lett.* **2006**, *418*, 448.
(35) Krisnamurthi, V.; Nagasha, K.; Marate, V. R.; Mathur, D. *Phys. Rev. A* **1991**, *44*, 5460.
(36) Cossart, D.; Cossart-Magos, C. *Chem. Phys. Lett.* **1996**, *250*, 128.
(37) Cossart, D.; Robbe, J. M. *Chem. Phys. Lett.* **1999**, *311*, 248.
(38) Belic, D. S.; Yu, D. J.; Siari, A.; Defrance, P. *J. Phys. B* **1997**, *30*, 5535.
(39) Kim, Y. K.; Irikura, K. K. *J. Res. Natl. Inst. Stand. Technol.* **2001**, *105*, 285.
(40) Larsson, M.; Baltzer, P.; Svensson, S.; Wannberg, B.; Martensson, N.; Naves de Brito, A.; Correia, N.; Keane, M. P.; Carlsson-Goethe, M.; Karlsson, L. *J. Phys. B* **1990**, *23*, 1175.
(41) Huber, K. P.; Herzberg, G. *Molecular Spectra and Molecular Structure IV. Constants of Diatomic Molecules*; Van Nostrand Reinhold; New York, 1979.
(42) Dawber, G.; McConkey, A. G.; Avaldi, L.; McDonalds, M. A.; King, G. C.; Hall, R. I. *J. Phys. B* **1994**, *27*, 2191.

JP712011T